FTIR-assisted electroreduction of CO_2 and H_2O to CO and H_2 by electrochemically deposited copper on oxidized graphite felt

Manuel E. G. Winkler[1,*], Ricardo Henrique Gonçalves[1], Adley Forti Rubira[1,*]

[1]Department of Chemistry, State University of Maringá, Av. Colombo 5790, CEP 87020-900, Maringá, PR, Brazil

[*]*Corresponding authors:* manuelgw@gmail.com, afrubira@gmail.com

1. LIST OF FIGURES

2. LIST OF TABLES

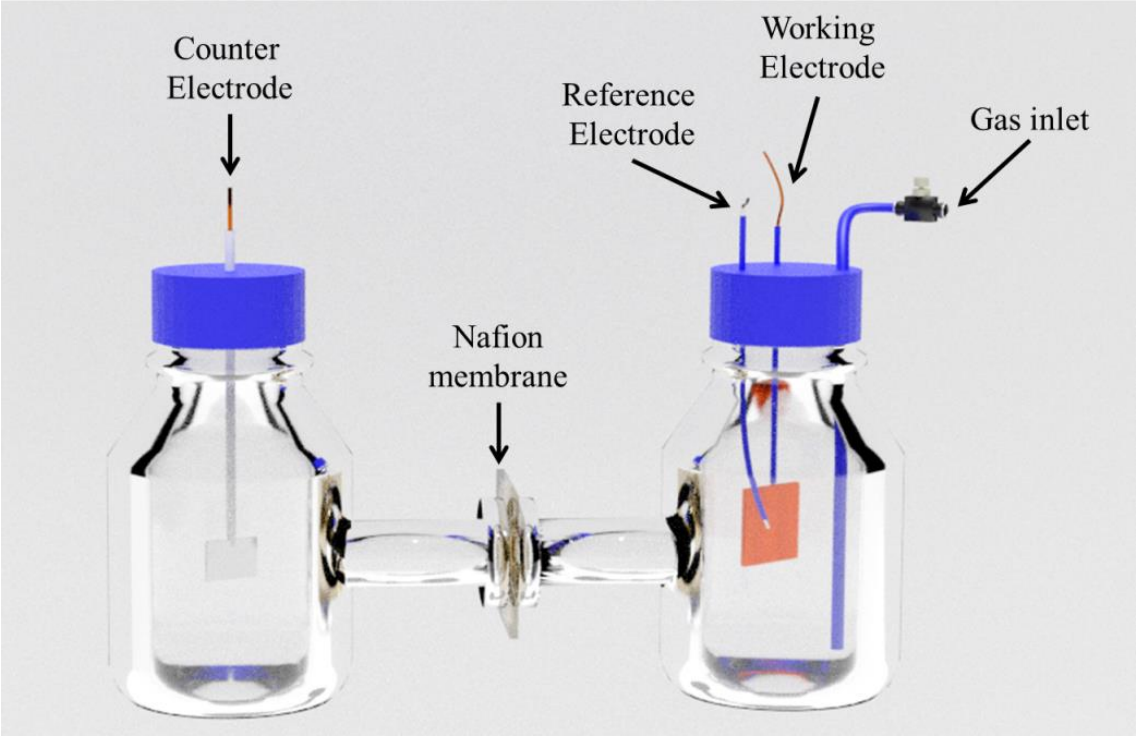

Figure S1. H-type electrochemical cell used in the experiments.

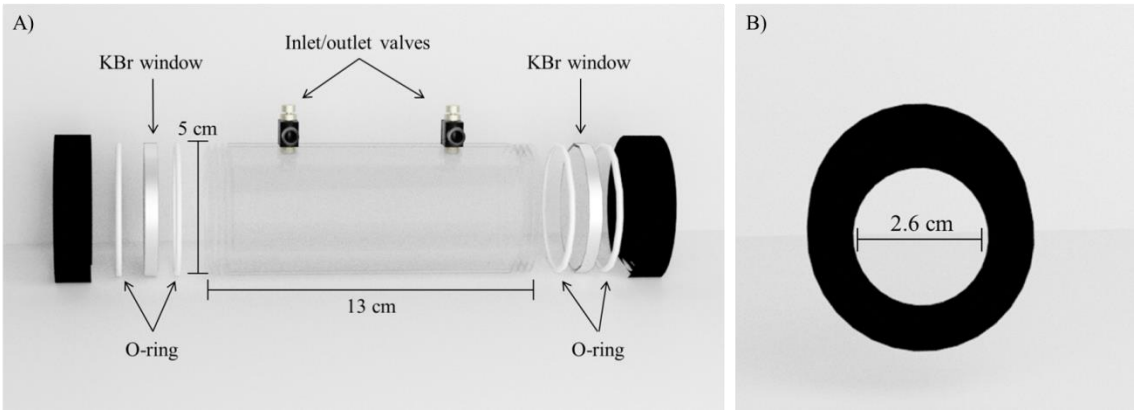

Figure S2. Short-path gas cell used for FTIR measurements.A) Side and B) front-view.

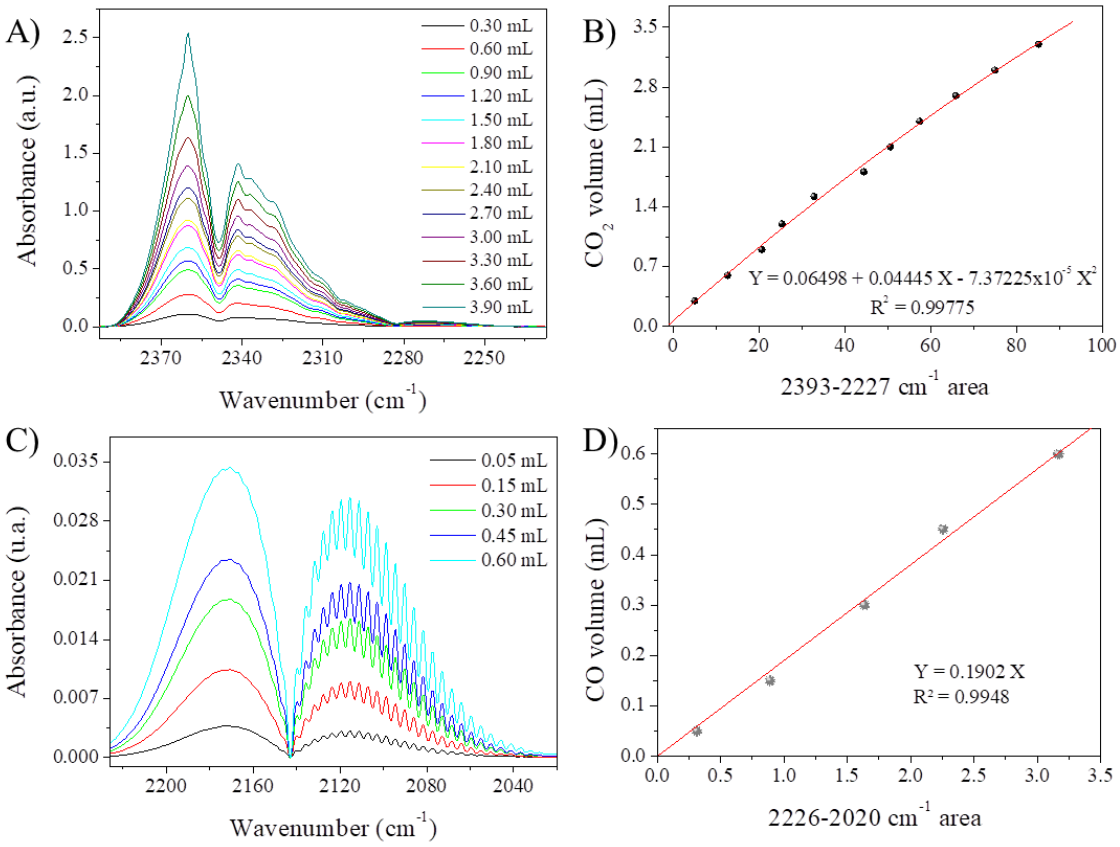

Figure S3. A) FTIR spectra of different volumes of CO_2. B) CO_2 analytical curve. C) FTIR spectra of different volumes of CO. D) CO analytical curve.

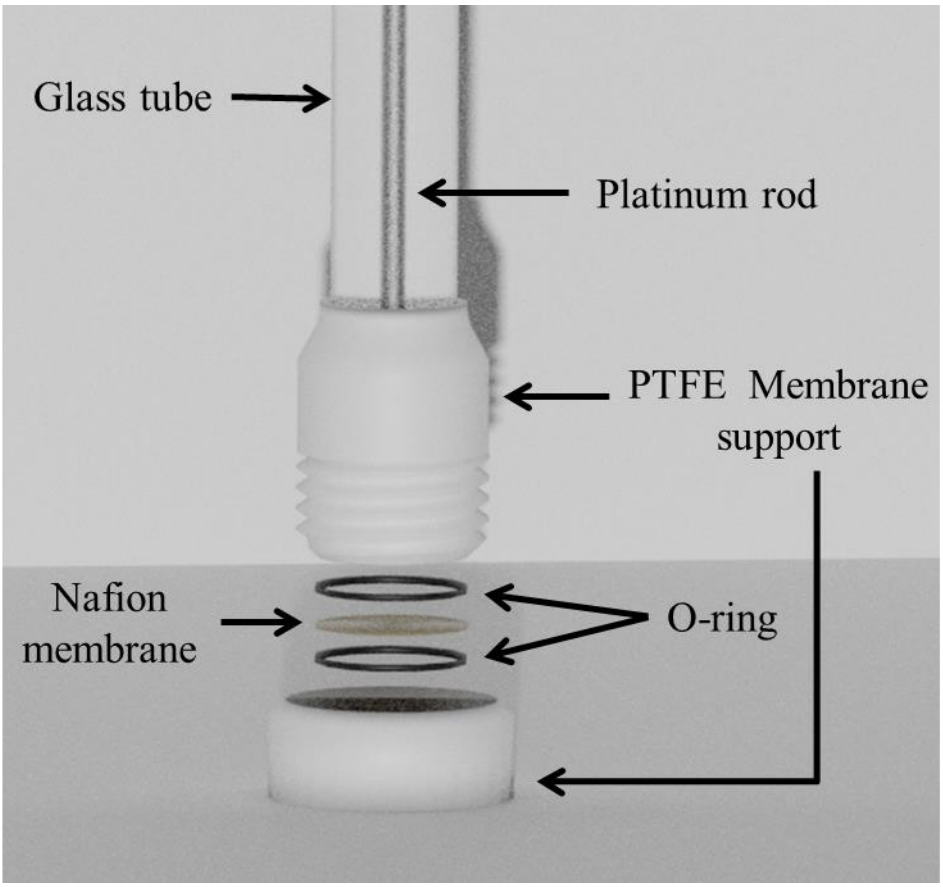

Figure S4. Counter electrode compartment in the electrochemical cell developed for FTIR analysis of the generated gaseous products.

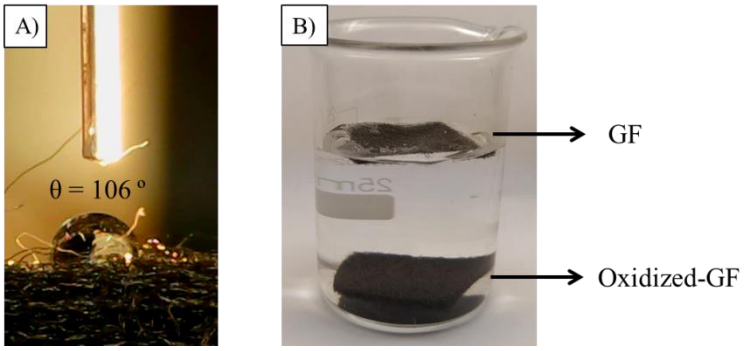

Figure S5. A) Graphite Felt/Water contact angle and B) wettability of graphite felt and Oxidized-graphite felt (OGF).

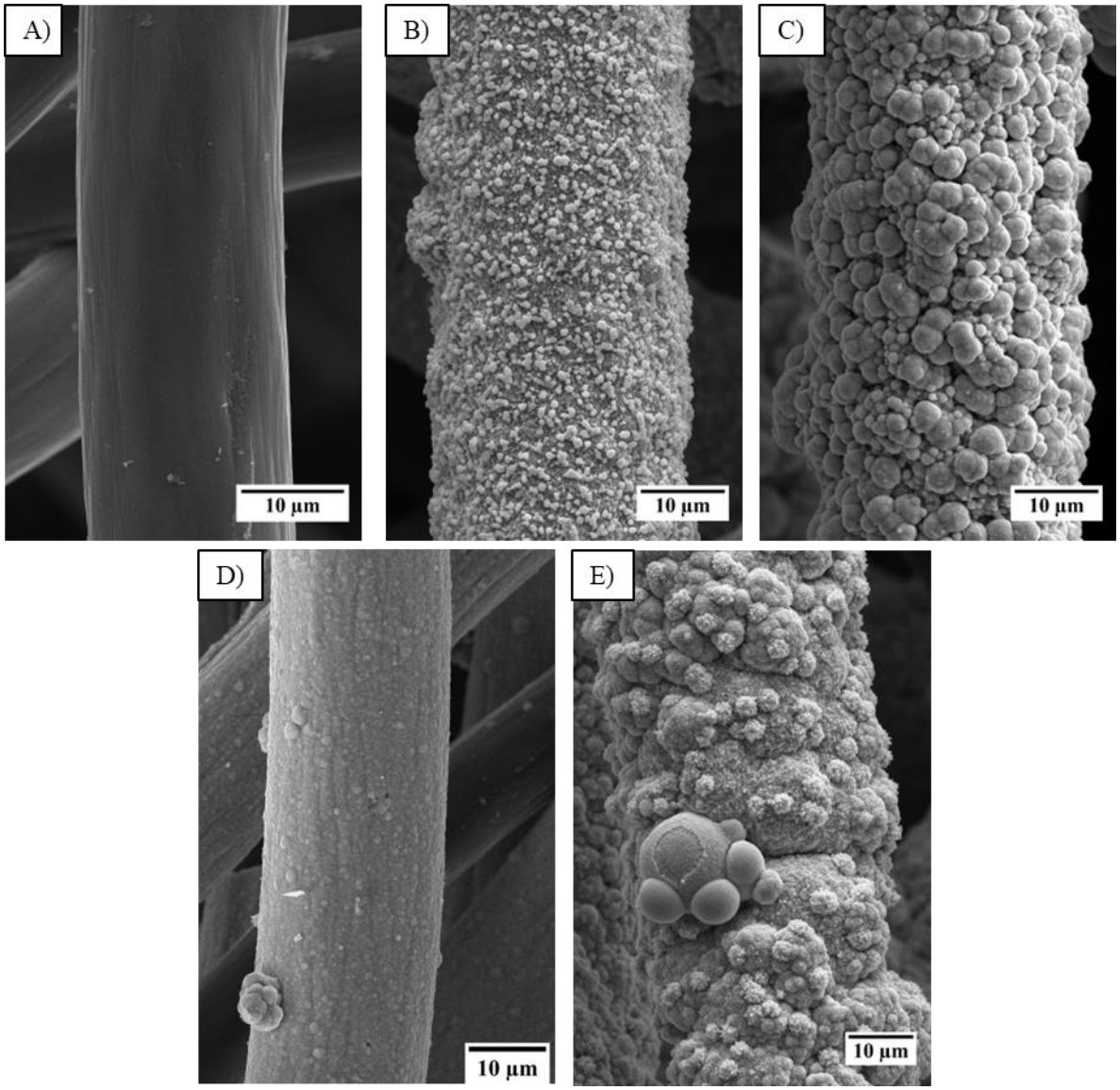

Figure S6. Low magnification images of the surface of A) Graphite felt, B) Cu-OGF pH 4, C) Cu-OGF pH 6, D), Cu-OGF pH 8, and E) Cu-OGF pH 10.

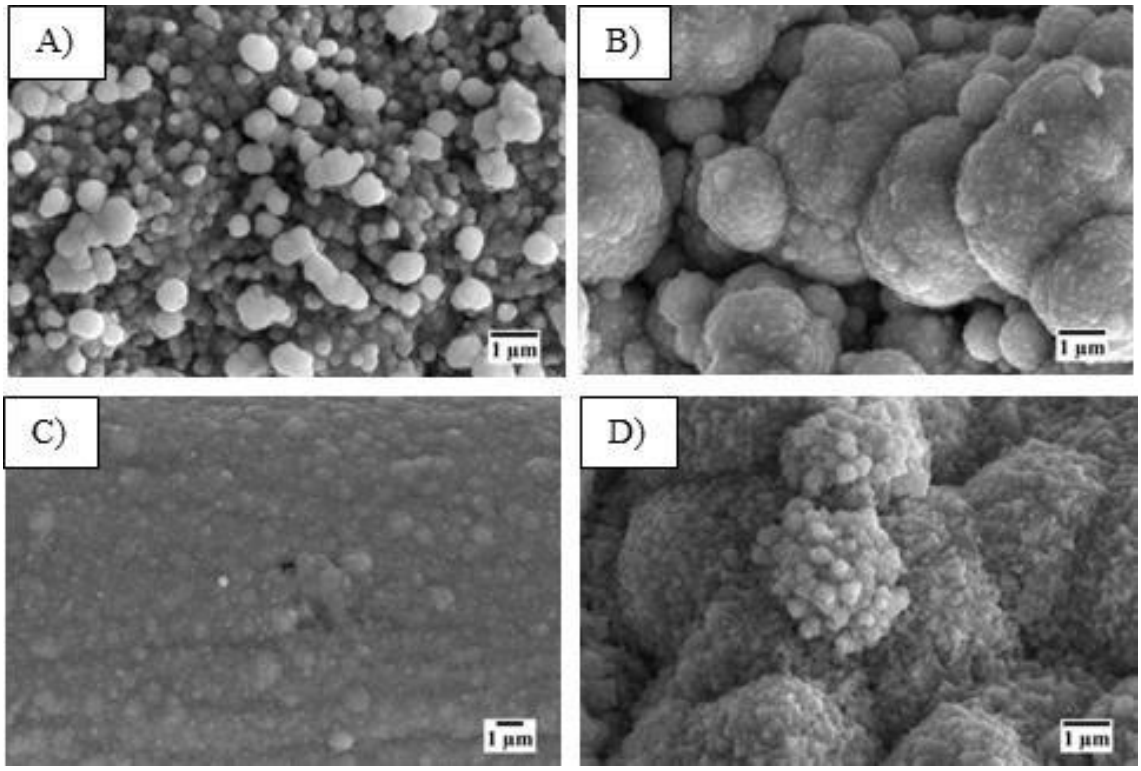

Figure S7. High magnification SEM images of the surface of A) Cu-OGF pH 4, B) Cu-OGF pH 6, C) Cu-OGF pH 8, and D) Cu-OGF pH 10.

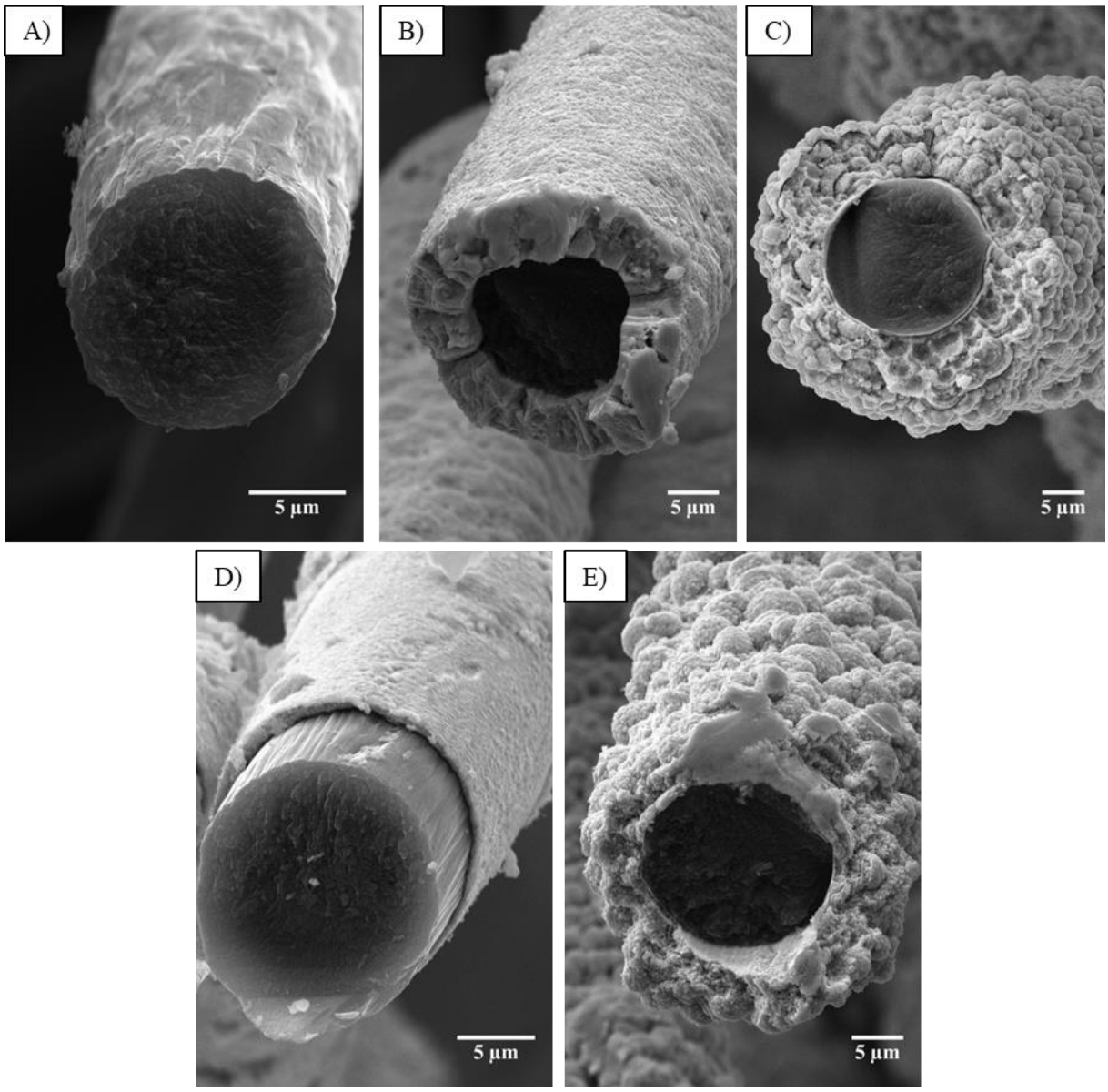

Figure S8. Cross-section SEM images of A) Graphite felt, B-E) Cu-OGF electrodes prepared in pH 4.0, 6.0, 8.0, and 10, respectively.

Table S1. Copper shell thickness of Cu-OGF electrodes measured by the cross-section SEM images.

Electrodepositionp H	Copper shell thickness (µm)
2.0	2.2
4.0	5.9
6.0	9.2
8.0	1.1
10.0	6.1

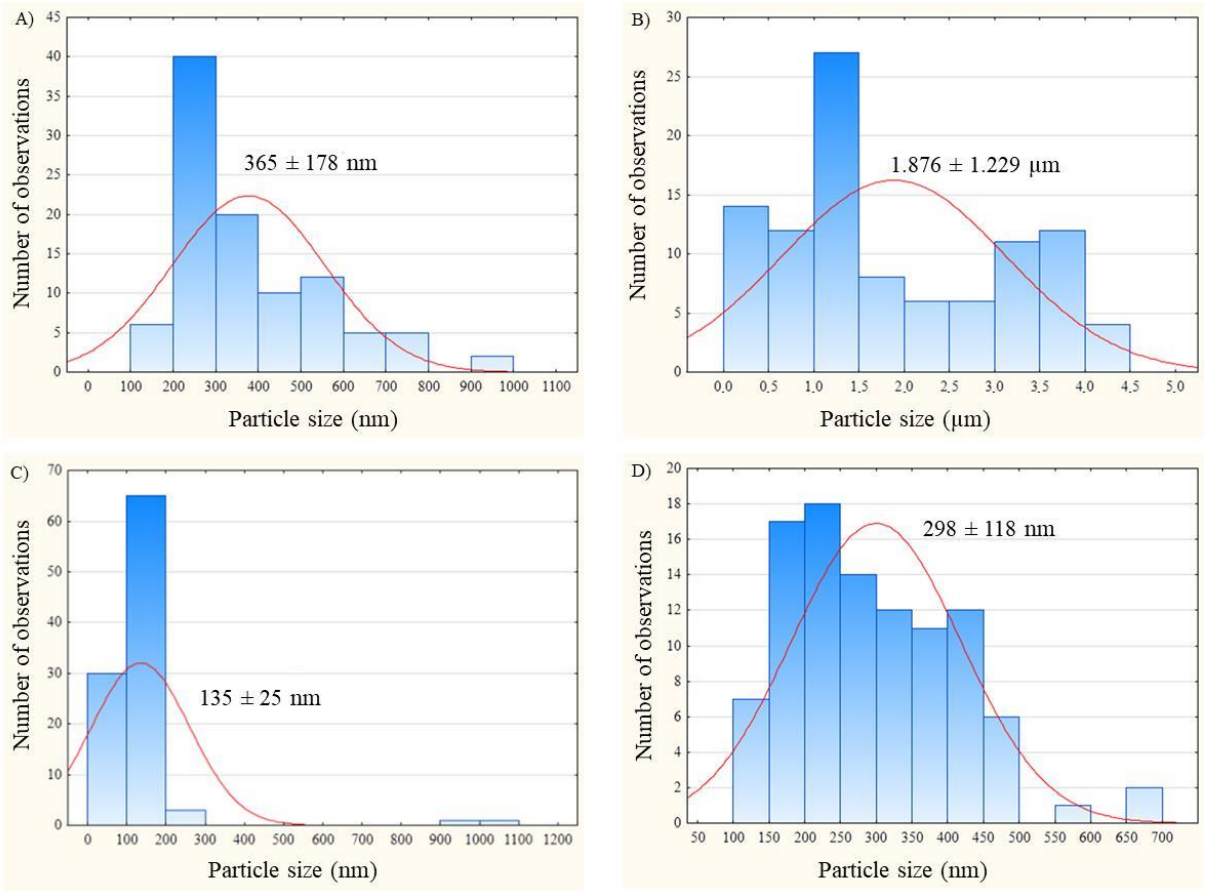

Figure S9. Size distribution of copper particles on the surface of A) Cu-OGF pH 4, B) Cu-OGF pH 6, C) Cu-OGF pH 8, and D) Cu-OGF pH 10.

Table S2. XRD assignment of as-prepared Cu-OGF pH 2.

2θ (º)	Assignment	Plane	Relative Intensity (%)
26.3	Graphite	(002)	21.17
36.7	Cu_2O*	(111)	14.57
42.5	Cu_2O*	(200)	4.73
43.6	Cu*	(111)	100
50.7	Cu*	(200)	45.26
61.5	Cu_2O*	(220)	3.35
73.7	Cu_2O*	(311)	4.23
74.3	Cu*	(220)	22.78

*JCPDS 03-065-3288;

*JCPDS 00-004-0836.

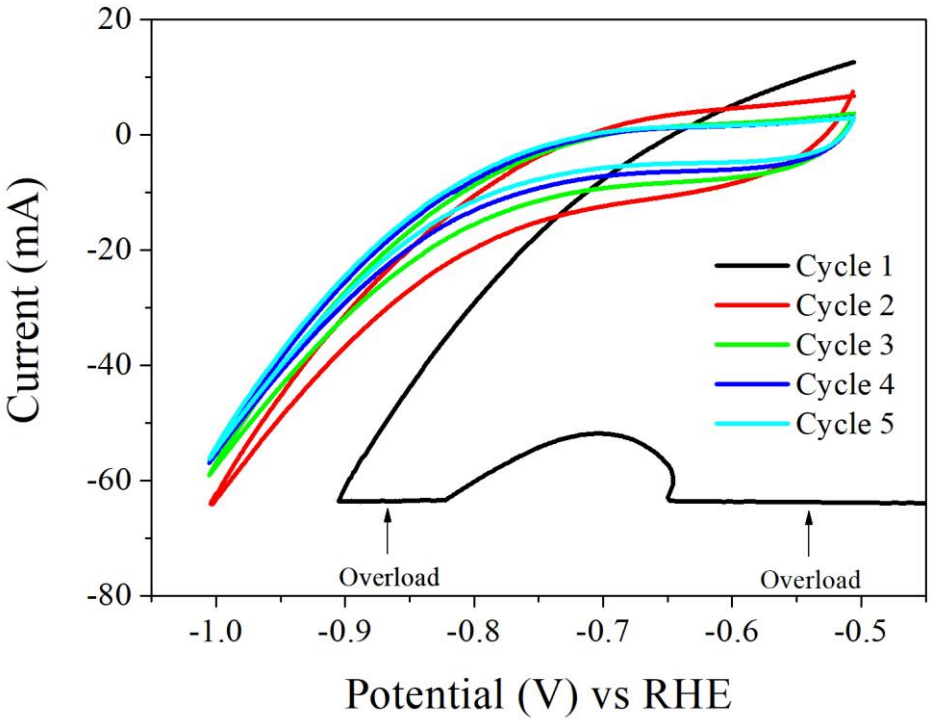

Figure S10. First five cycles of Cu-OGF pH 2 electrode voltammetry in 0.1 M $NaHCO_3$ and 0.1 M KCl N_2-saturated. Scan rate 20 $mV.s^{-1}$.

Table S3. XRD assignment of reduced Cu-OGF pH 2.

2θ (º)	Assignment	Plane	Relative Intensity (%)
26.3	Graphite	(002)	6.28
36.7	Cu_2O*	(111)	2.30
43.6	Cu*	(111)	100
50.7	Cu*	(200)	28.16
74.3	Cu*	(220)	14.82

*JCPDS 03-065-3288;

*JCPDS 00-004-0836.

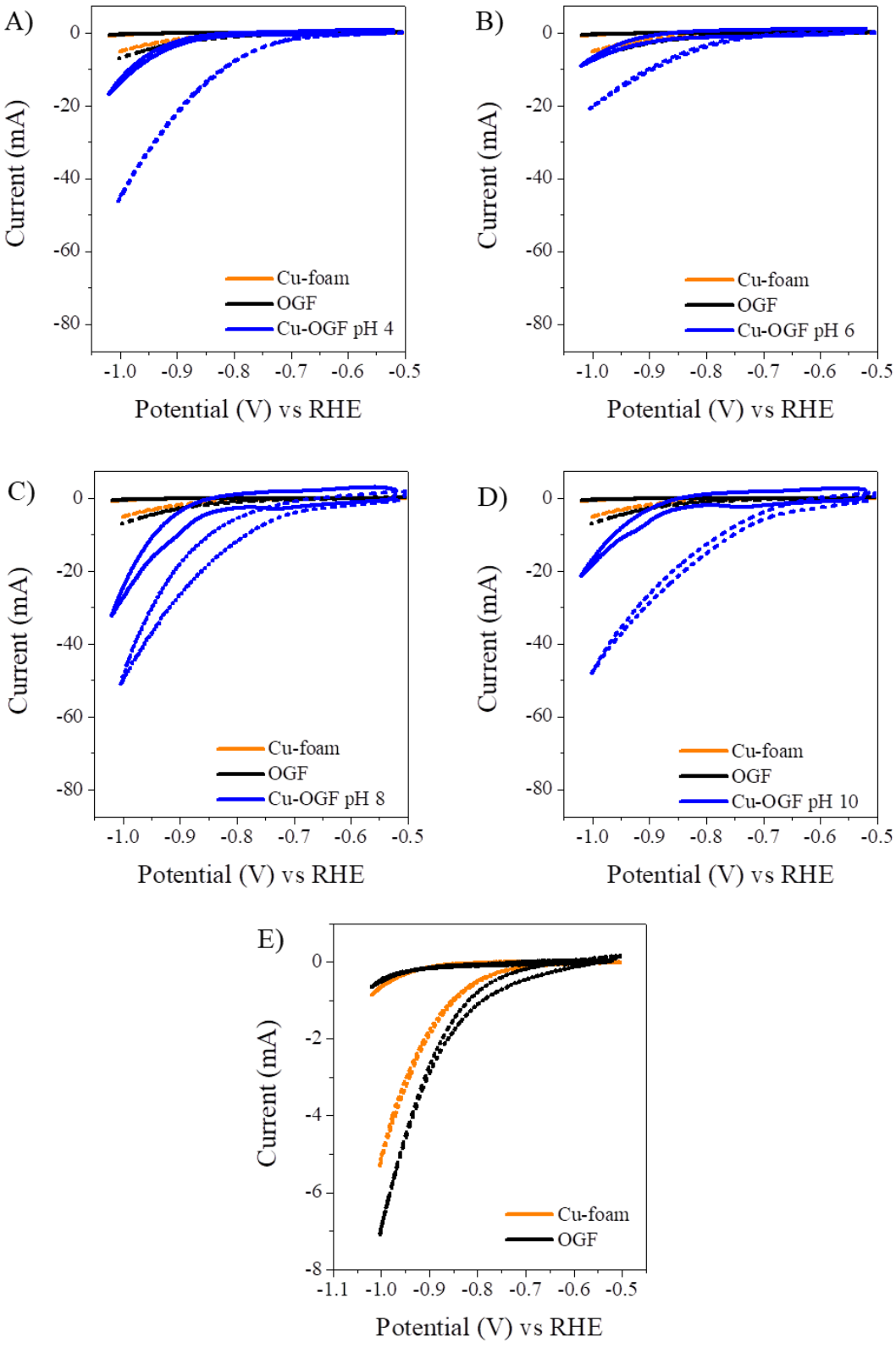

Figure S11. Cyclic voltammograms of the A) Cu-OGF pH 4, B) Cu-OGF pH 6, C) Cu-OGF pH 8, D) Cu-OGF pH 10 E) OGF and Cu-foam electrodes in 0.1 $NaHCO_3$ and 0.1 M KCl N_2-saturated and CO_2-saturated. Scan rate 1 $mV.s^{-1}$.

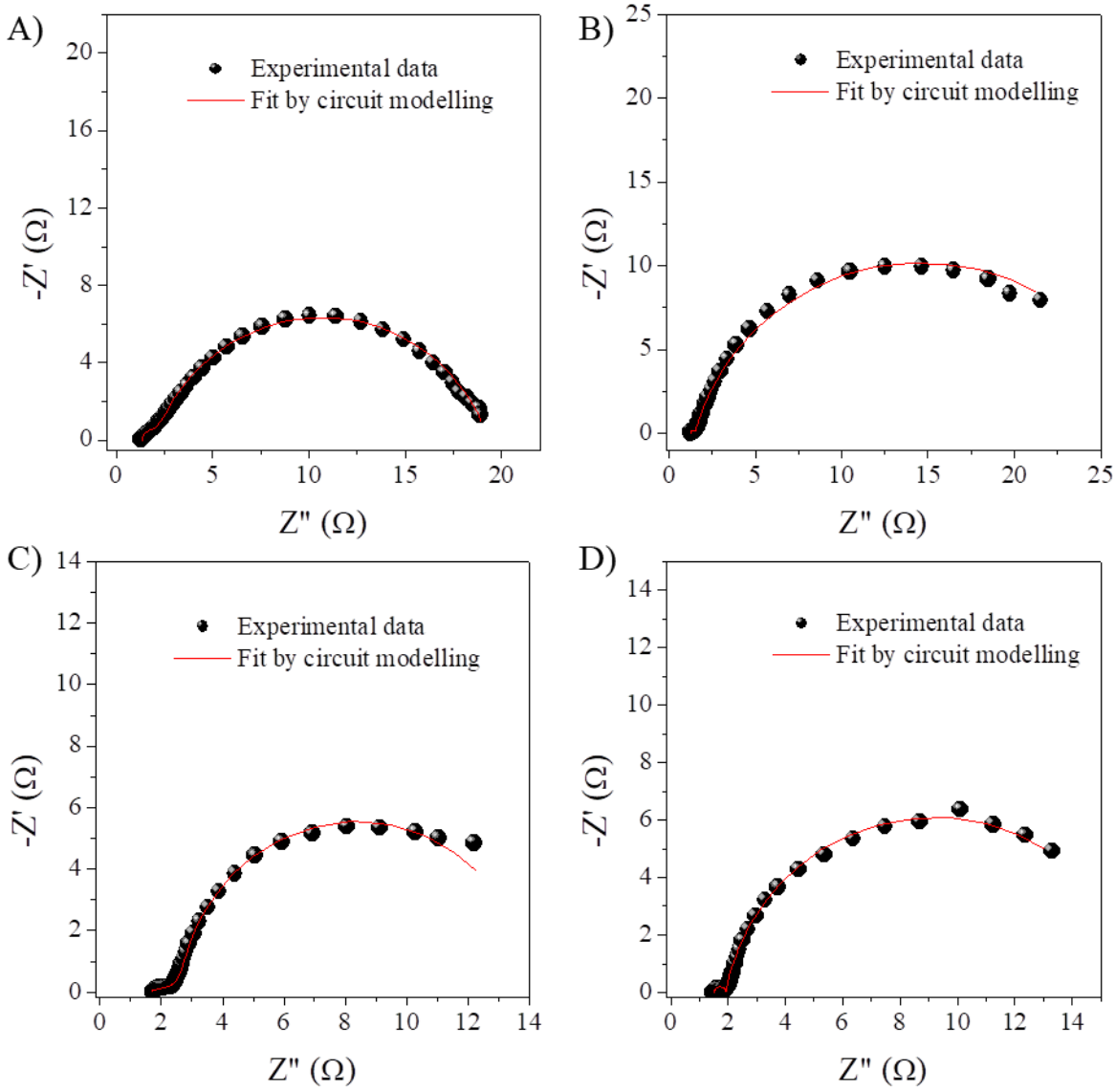

Figure S12. Nyquist diagrams and equivalent circuit simulation data of the electrodes A) Cu-OGF pH 4, B) Cu-OGF pH 6, C) Cu-OGF pH 8, and D) Cu-OGF pH 10 in 0.1 M $NaHCO_3$ and 0.1 M KCl CO_2-saturated at -0.68 V vs RHE.

Table S4. Equivalent circuit simulation data of Cu-OGF pH 2, Cu-OGF pH 4, Cu-OGF pH 6, Cu-OGF pH 8, and Cu-OGF pH 10 electrodes.

Electrode	Rs (Ω)	Rct (Ω)	Cdl (mF)	Rp (Ω)	CPE (mF)	Goodness of fit
Cu-OGF pH 2	1.267 ± 0.008	0.198 ± 0.029	28.90 ± 6.08	9.239 ± 0.144	174.00 ± 6.00	1.91 x 10-4
Cu-OGF pH 4	1.282 ± 0.032	0.972 ± 0.116	2.466 ± 0.40	17.030 ± 0.373	30.55 ± 0.17	2.29 x 10-4
Cu-OGF pH 6	1.225 ± 0.004	0.269 ± 0.008	5.757 ± 0.34	26.180 ± 0.569	321.00 ± 1.48	2.72 x 10-4
Cu-OGF pH 8	1.351 ± 0.034	0.973 ± 0.117	2.47 ± 0.47	17.030 ± 0.370	30.00 ± 0.20	1.12 x 10-3
Cu-OGF pH 10	1.520 ± 0.013	0.502 ± 0.002	4.15 ± 0.43	13.880 ± 0.005	763.00 ± 0.01	3.24 x 10-4

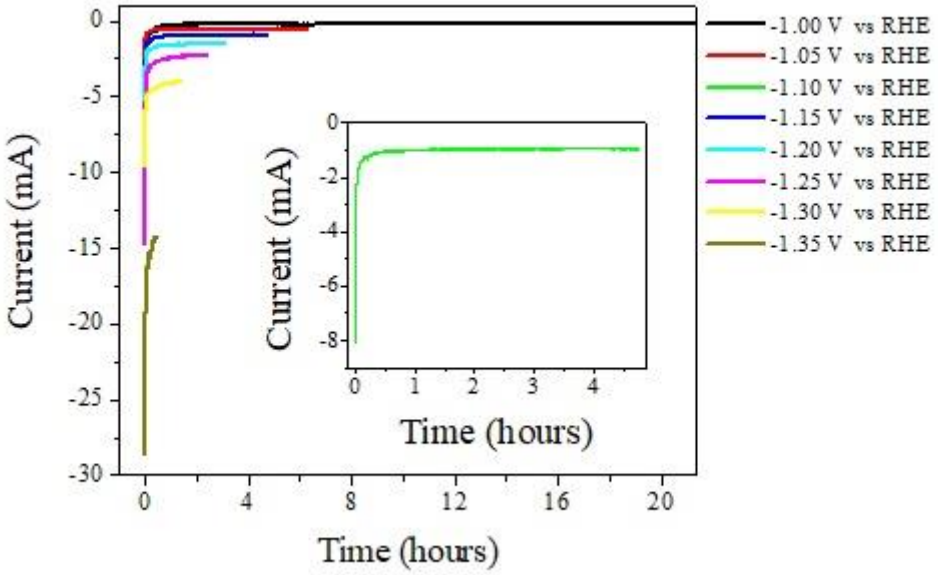

Figure S13. Chronoamperometry curves of Cu-OGF pH 2 electrode at different applied voltages in CO_2-saturated $NaHCO_3$-saturated electrolyte.

Table S5. Chronoamperometry results at different applied voltages and faradaic efficiency towards CO, H_2 and total.

Potential (V) vs RHE	Total volume (mL)	Analyzed volume (mL)	Q (C)	n CO_2 (mmol)	n CO (mmol)	FE CO (%)	FE H_2 (%)	Total FE (%)
-1.00	5.20	5.20	17.01	0.135	0.0005	0.58	85.58	86.17
-1.05	5.10	5.10	13.12	0.151	0.0008	1.11	80.39	81.50
-1.10	9.00	5.10	45.96	0.137	0.0026	1.92	50.87	52.79
-1.15	5.20	5.20	17.17	0.155	0.0032	3.54	61.65	65.19
-1.20	5.20	5.20	17.90	0.137	0.0029	3.13	78.09	81.22
-1.25	5.20	5.20	21.51	0.138	0.0030	2.73	64.57	67.31
-1.30	5.20	5.20	21.16	0.134	0.0030	2.76	69.38	72.15
-1.35	5.20	5.20	24.14	0.124	0.0019	1.49	69.61	71.10

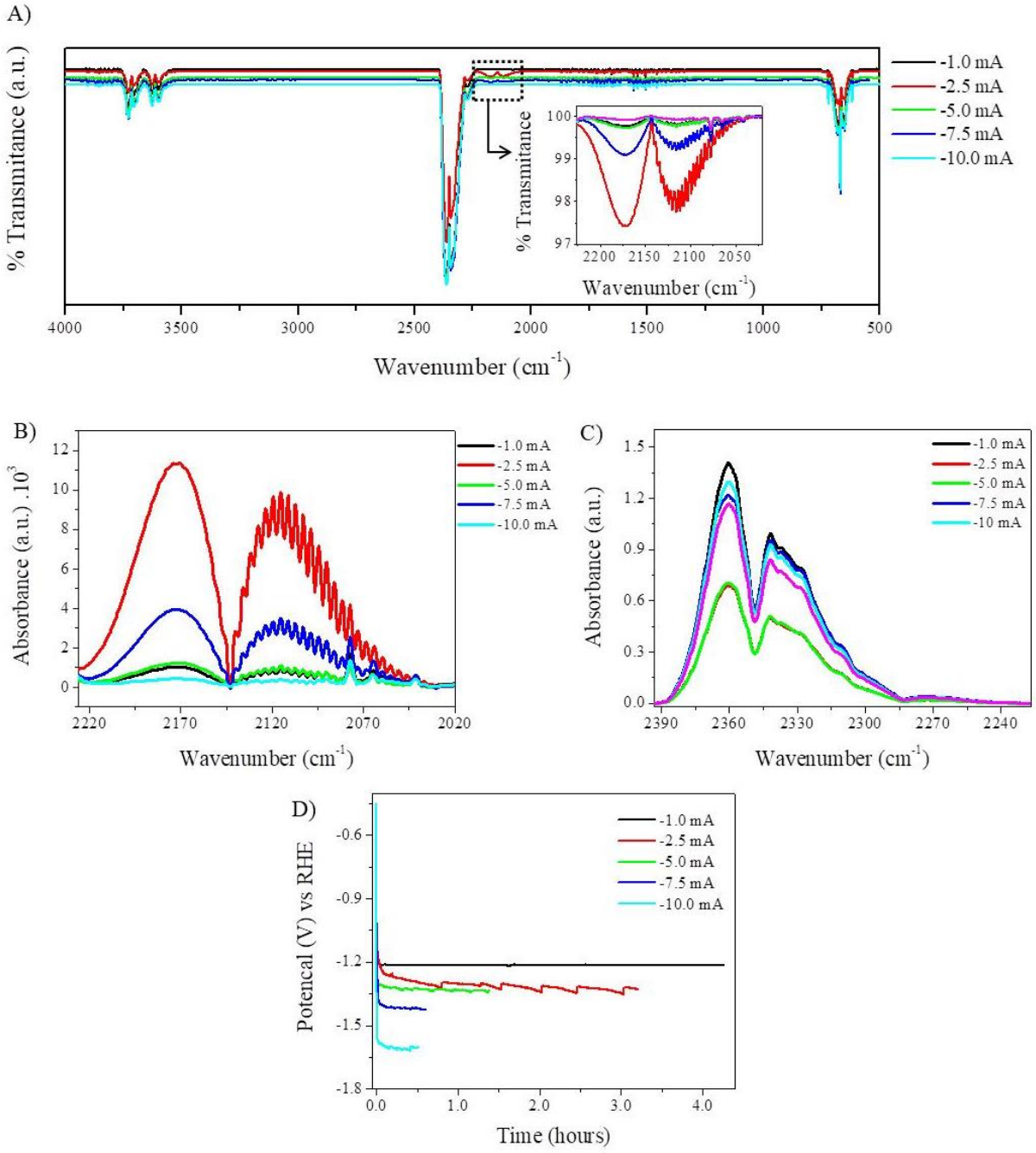

Figure S14. A) FTIR spectra of the produced gases at different currents at 4000-500 cm^{-1} (inset: 2226-2020 cm^{-1}), B) and C) absorption regions of carbon monoxide and carbon dioxide, respectively. D) Chronopotentiometric curves.

Table S6. Chronopotenciometry results at different currents and faradaic efficiency towards CO, H_2 and total.

Current (mA)	Total volume (mL)	Analyzed volume (mL)	Q (C)	n CO_2 (mmol)	n CO (mmol)	FE CO (%)	FE H_2 (%)	Total FE (%)
-1.0	4.90	4.90	15.33	0.124	0.0009	1.12	95.04	96.16
-2.5	5.00	5.00	28.89	0.064	0.0078	5.21	88.80	94.02
-5.0	4.70	4.70	24.99	0.064	0.0009	0.72	98.30	99.02
-7.5	6.40	5.00	16.42	0.119	0.0028	3.25	97.00	100.25
-10.0	5.00	5.00	18.41	0.116	0.0005	0.50	91.78	92.27

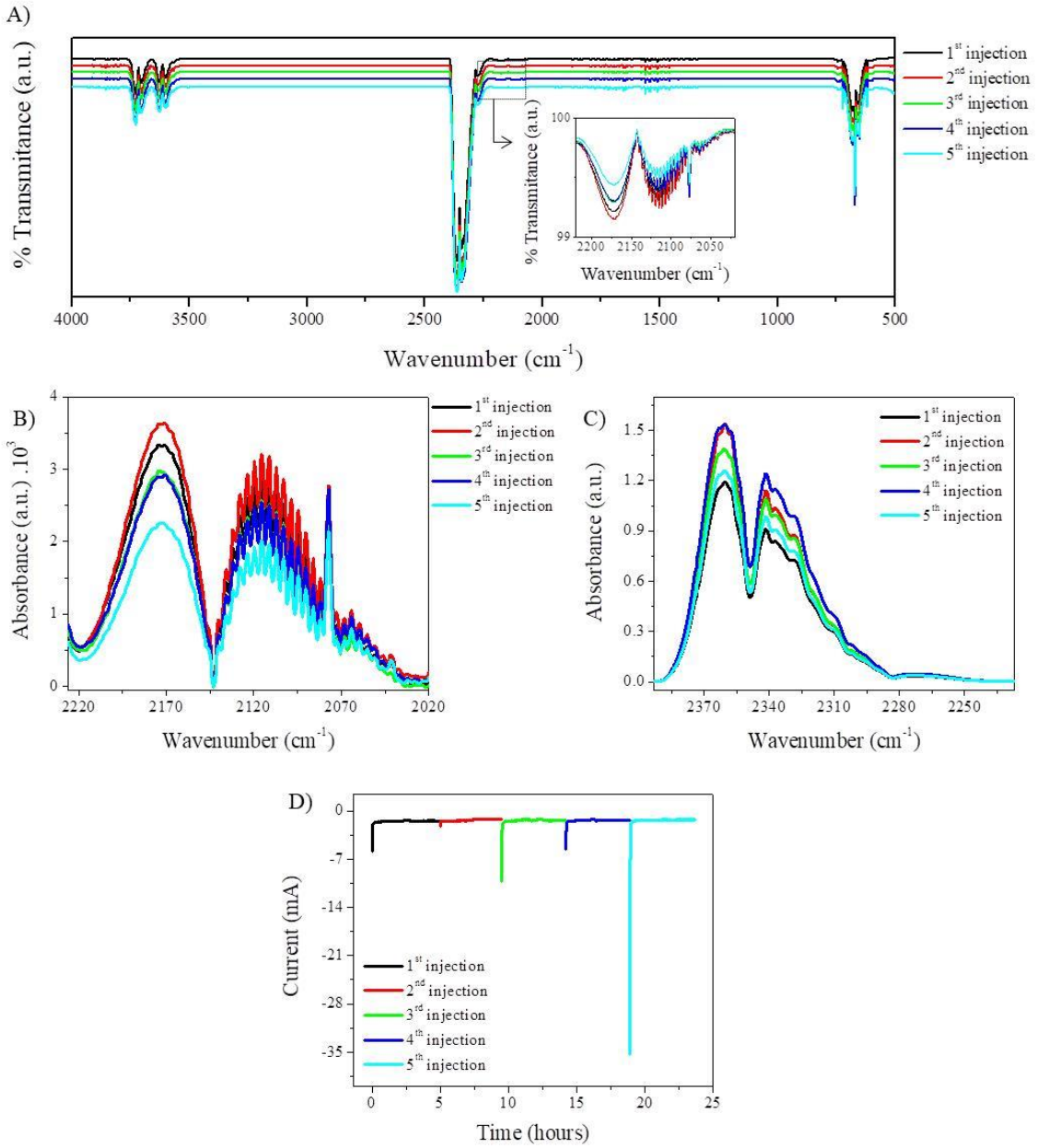

Figure S15. A) FTIR spectra of the produced gases at -1.15 V vs RHE at 4000-500 cm^{-1} (inset: 2226-2020 cm^{-1}), B) and C) absorption regions of carbon monoxide and carbon dioxide, respectively. D) Chronoamperometric curve.

Table S7. Chronoamperometric results at -1.15 V vs RHE and faradaic efficiency towards CO, H_2 and total.

Injection	Total volume (mL)	Analyzed volume (mL)	Q (C)	n CO_2 (mmol)	n CO (mmol)	FE CO (%)	FE H_2 (%)	Total FE (%)
1st	4.90	4.90	17.17	0.112	0.0024	2.67	97.03	99.70
2nd	11.90	5.20	48.24	0.112	0.0024	2.21	90.26	92.47
3rd	6.40	5.30	23.61	0.134	0.0026	2.57	78.89	81.45
4th	6.90	5.10	23.27	0.130	0.0021	2.36	85.75	88.11
5th	4.90	4.90	18.98	0.119	0.0017	1.72	81.29	83.01

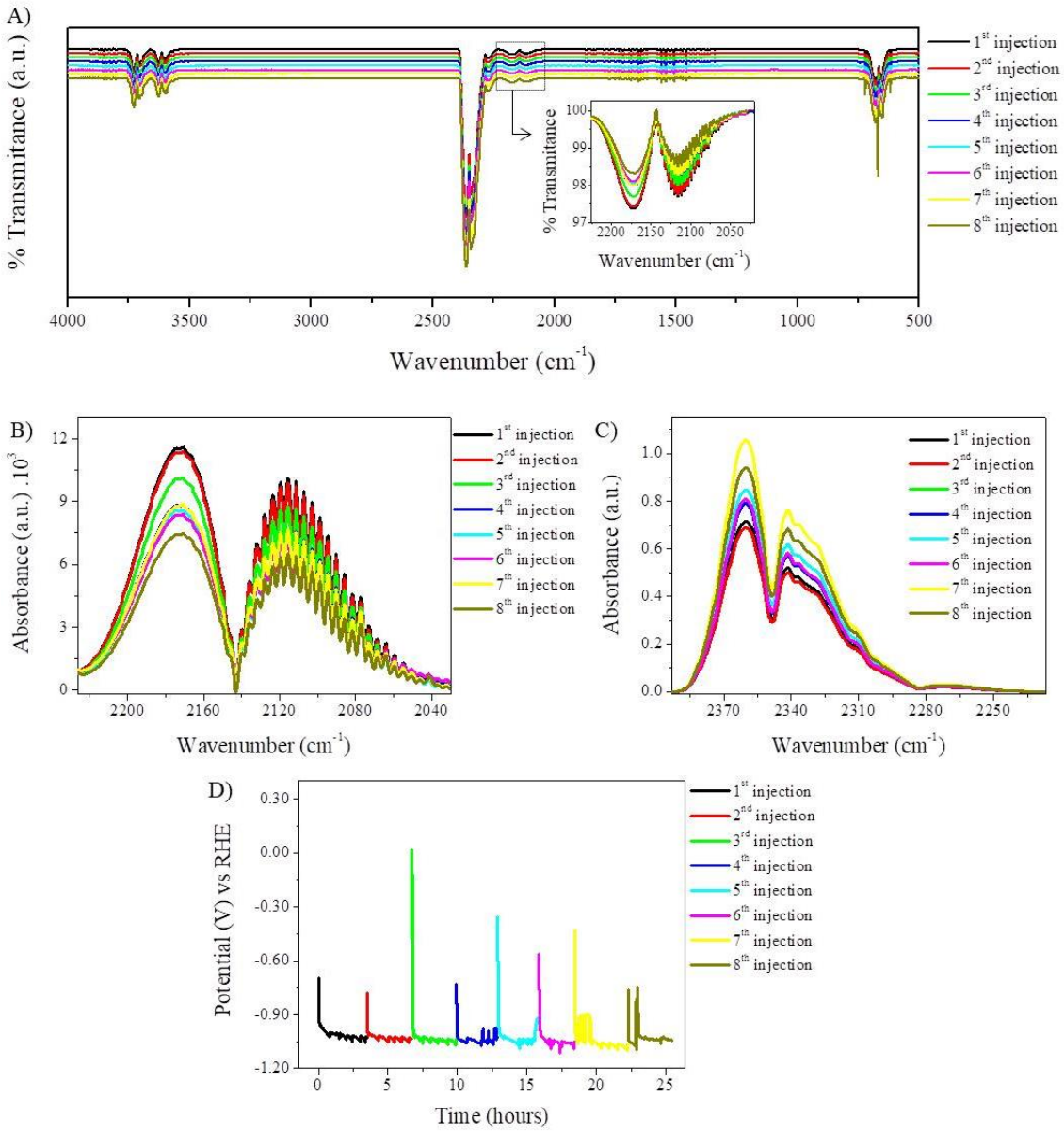

Figure S16. A) FTIR spectra of the produced gases at -2.5 mA at 4000-500 cm-1 (inset: 2226-2020 cm-1), B) and C) absorption regions of carbon monoxide and carbon dioxide, respectively. D) Chronopotenciometric curve.

Table S8. Chronopotenciometric results at -2.5 mA and faradaic efficiency towards CO, H_2 and total.

Injection	Total volume (mL)	Analyzed volume (mL)	Q (C)	n CO_2 (mmol)	n CO (mmol)	FE CO (%)	FE H_2 (%)	Total FE (%)
1st	5.00	5.00	31.79	0.066	0.008	4.88	79.02	83.89
2nd	5.00	5.00	28.89	0.064	0.008	5.21	88.80	94.02
3rd	5.00	5.00	28.74	0.070	0.007	4.68	85.61	90.29
4th	5.00	5.00	25.67	0.073	0.006	4.59	94.41	99.00
5th	5.00	5.00	25.29	0.079	0.006	4.46	91.19	95.65
6th	5.00	5.00	25.88	0.074	0.006	4.43	92.77	97.21
7th	5.80	5.80	30.06	0.097	0.006	3.93	86.37	90.30
8th	5.50	5.50	26.70	0.088	0.005	3.70	95.58	99.28

In order to compare with a standard sample, chronopotentiometric experiments for CO and H_2 quantification were performed using Cu-Foam of the same geometric dimensions (4.0 cm x 1.0 cm x 0.2 cm) as the working electrode. Chronopotentiometric curves are presented in Figure S17 (A), and FTIR spectra in Figure S17 (B-E). From these results, the faradaic efficiencies for CO and H_2 were calculated, and the results are shown in Table S9. As can be seen from these results, Cu-foam requires a much higher current than Cu-OGF pH 2 for CO and H_2 production, with low faradaic efficiencies (0.55 % and 3.19 %, respectively). In addition, as can be seen from the expanded FTIR spectrum, the presence of a characteristic C-H stretching peak at 3000 cm^{-1} indicates low selectivity for CO and H_2 (Figure S17 C).

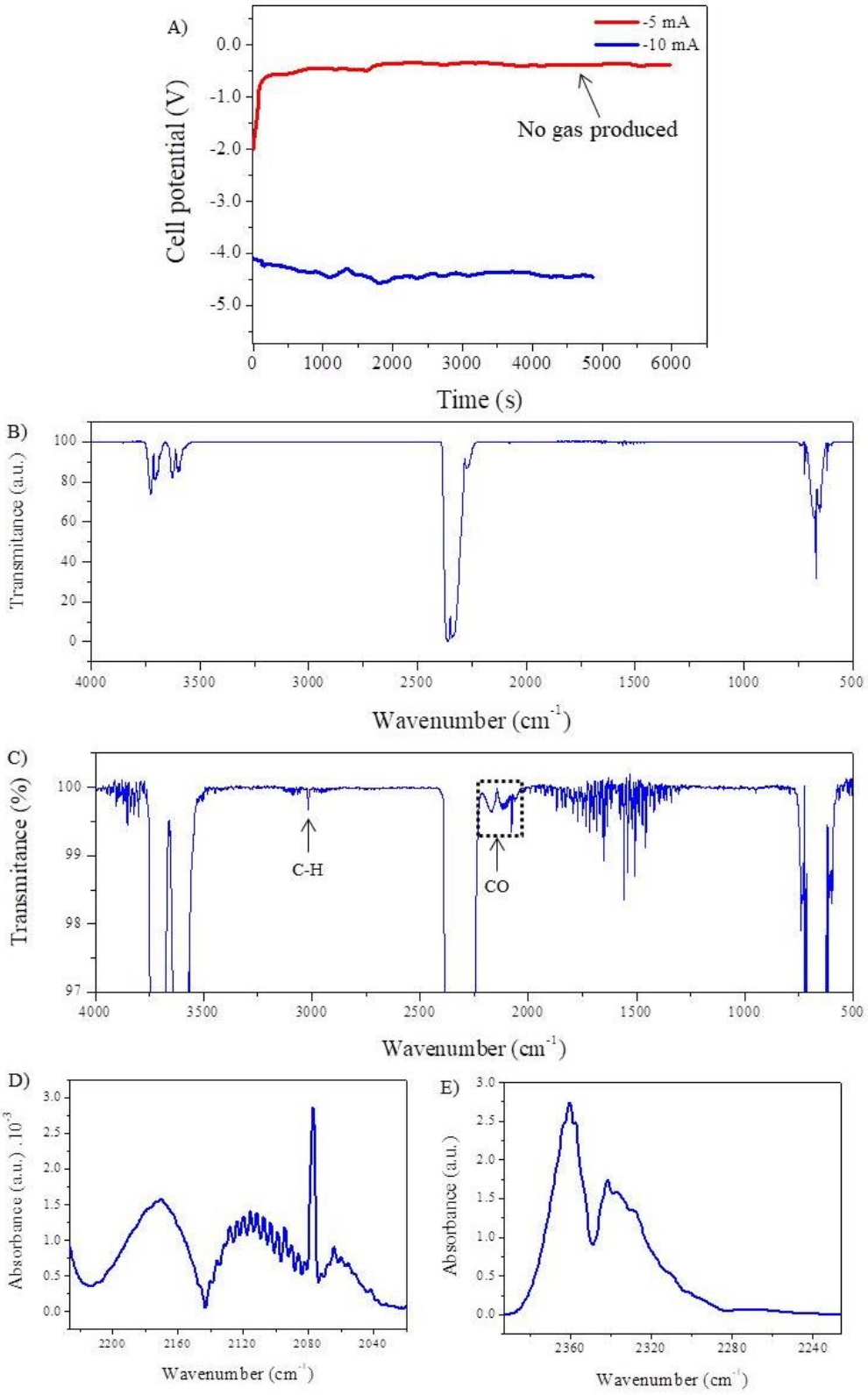

Figure S17. A) Chronopotenciometric curves of Cu foam electrode at -5.0 mA and -10 mA in a two-electrode configuration cell; B-C) Full-range and expanded FTIR spectra of the produced gas at -10 mA, respectively; and D) absorption region of carbon monoxide and E) carbon dioxide.

Table S9. Chronopotenciometric results at -10.0 mA and faradaic efficiency towards CO, H_2 and total for Cu-foam electrode.

Total volume (mL)	Analyzed volume (mL)	Q (C)	n CO_2 (mmol)	n CO (mmol)	FE CO (%)	FE H_2 (%)	Total FE (%)
5.20	5.20	45.85	0.204	0.0013	0.55	3.19	3.74

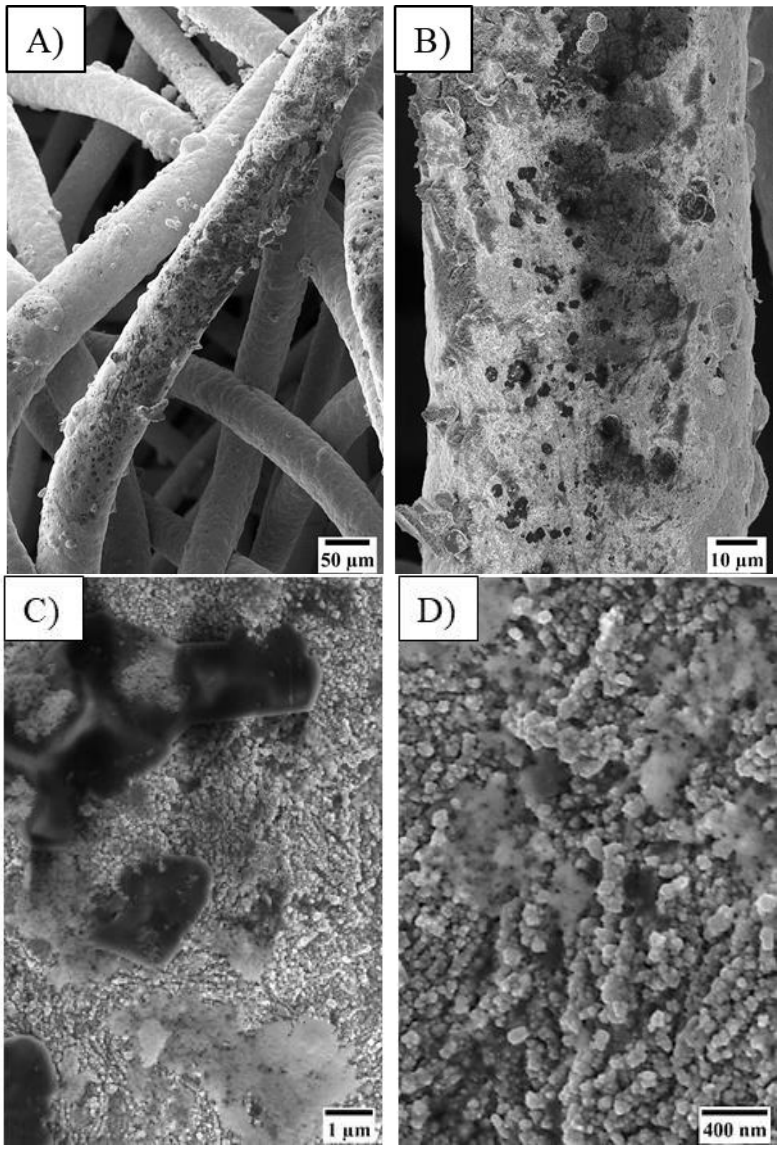

Figure S18. A-B) Low and C-D) high-magnification SEM images of post-electrolysis Cu-OGF pH 2 electrode.

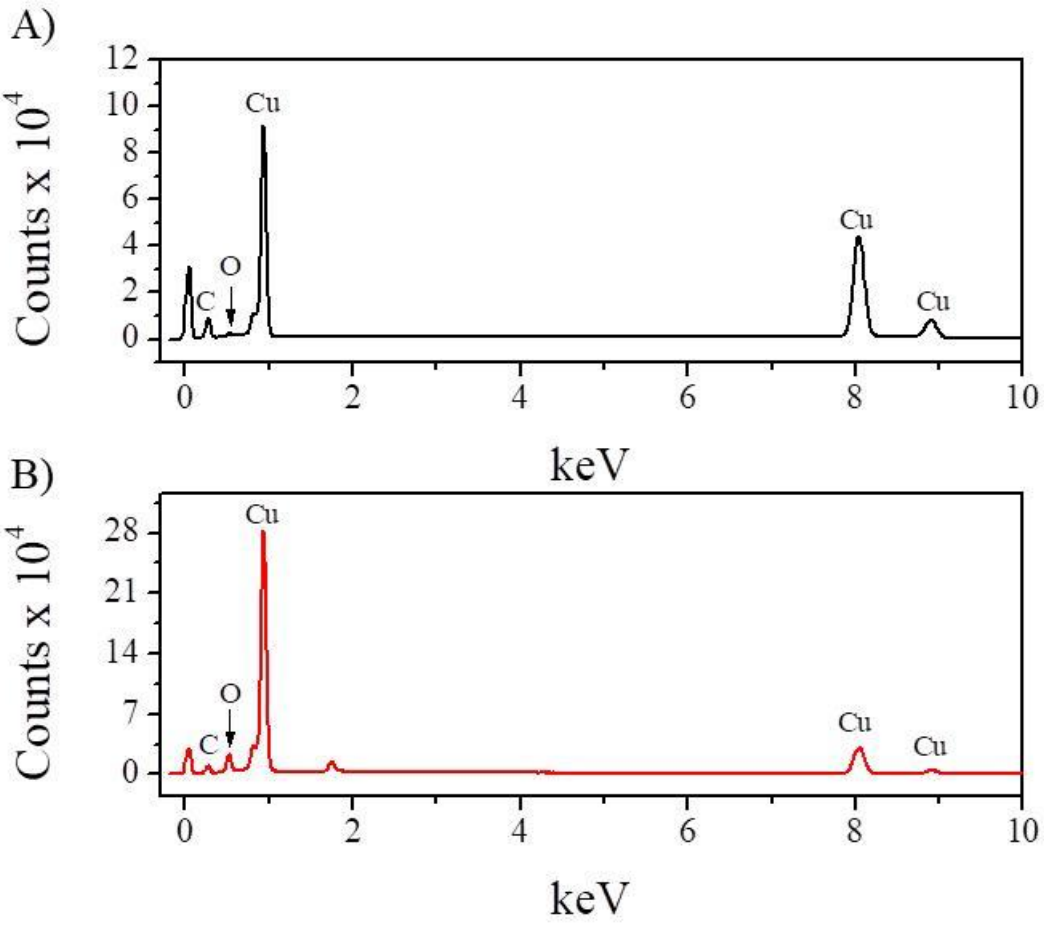

Figure S19. EDX spectra of A) pre and B) post-electrolysis Cu-OGF pH 2 electrode.